Supporting Information

Montoyo *et al.* 10.1073/pnas.0810796106

SI Text

Typing of Mice. Mice were genotyped by isolating tail DNA followed by use in the PCR with the following oligonucleotide primers (shown in supporting information (SI) Fig. S1):

1. Presence of wild-type allele: primer 3 (5′ CCA TGG CTT TCT CTC AGC GGC GAT GAC 3′) plus primer 6 (5′ TTA TGT GGA GAT GGA AAA CAA CCA TGT ACA 3′).

2. Presence of the floxed FcRn allele: primer 1 (5′ GCA AAG AGT GAA AGA GGA AGG AGC CTG CAA 3′) plus primer 2 (5′ CTC TTG CAA AAC CAC ACT GCT CGA 3′); primer 4 (5′ TGC CCA CTG CAG CCT TTC G 3′) plus primer 5 (5′ GAA GGG AAA CTG AAG CAG GC 3′); primer 3 (5′ CCA TGG CTT TCT CTC AGC GGC GAT GAC 3′) plus primer 6 (5′ TTA TGT GGA GAT GGA AAA CAA CCA TGT ACA 3′) (note that the insertion of a ≈100-bp fragment containing the loxP site allows this allele to be distinguished from the wild-type allele).

3. Deletion of floxed allele: primer 1 (5′ GCA AAG AGT GAA AGA GGA AGG AGC CTG CAA 3′) plus primer 6 (5′ TTA TGT GGA GAT GGA AAA CAA CCA TGT ACA 3′).

The presence of the Tie2-Cre recombinase gene was also analyzed using tail DNA and the PCR with the Cre-specific primers 5′ CGC ATA ACC AGT GAA ACA GCA TTG C 3′ and 5′ CCC TGT GCT CAG ACA GAA ATG AGA 3′.

Surface Plasmon Resonance. The approximate equilibrium dissociation constant for the very weak interaction of the human IgG1 mutant H435A and mouse FcRn was estimated using the following formula:

$$\mathrm{Req} = \frac{\mathrm{Rmax.[FcRn]}}{K_D + [\mathrm{FcRn}]}$$

where Req = equilibrium binding signal (in resonance units, RU) at a given concentration of FcRn, and Rmax = binding signal (in RU) when all binding sites of ligand on the flow cell are occupied. In these analyses, wild-type human IgG1 and the H435A mutant (both specific for hen egg lysozyme) (1) were immobilized using amine coupling chemistry at densities of 536 and 588 RU, respectively. Because the low affinity of the H435A-mouse FcRn interaction precludes determination of the signal level (in RU) when all binding sites of IgG are occupied by FcRn, hen egg lysozyme was injected at a concentration of 100 μg/ml or 150 μg/ml (saturating for binding) to estimate the amount of active H435A mutant on the flow cell. This binding signal was then used, with the maximal binding signals obtained from injecting saturating concentrations of either hen egg lysozyme (as described) over IgG1 and H435A or mouse FcRn (1 mg/ml) over the flow cell coupled with wild-type human IgG1, to estimate the hypothetical maximal signal in RU for FcRn binding to the H435A-coupled flow cell. This was followed by injections of soluble, recombinant mouse FcRn at concentrations up to 1 mg/ml (≈16.67 μM) to determine the equilibrium binding signals (Req) at different analyte concentrations.

Preparation of Samples for Immunohistochemistry. For analyses of FcRn expression in endothelium of spleens and livers, mice were injected intravenously with 50–100 μg Alexa 647-labeled IgG1 (MST-HN or H435A mutants). Three hours later, mice were perfused with heparinized saline (pH 6.0) and organs were harvested and frozen. Sections of 5 μm were cut using a Leica CM3050 S cryostat. Sections were rehydrated in PBS, fixed with 3.4% paraformaldehyde, and permeabilized with 0.05% saponin. Following blocking with 5% BSA/PBS (bovine albumin does not bind detectably to mouse/rat FcRn) (ref. 2 and unpublished data) and treatment with 5 μg/ml anti-FcγRIIB/III (2.4G2) antibody, sections were incubated with anti-endomucin (V.7C7) antibody (3) (0.7 μg/ml; Santa Cruz Biotechnology or generously provided by Dr. D. Vestweber, Max Planck Institute of Molecular Biomedicine, Röntgenstrasse 48149 Münster, Germany) in 1% BSA/PBS at pH 6.8 and bound antibody detected using Alexa 488-labeled goat anti-rat IgG (Invitrogen/Molecular Probes).

To detect FcRn in intestinal epithelium, mice were perfused with heparinized saline and duodena isolated, frozen, and sectioned. Sections were prepared as above and stained with a combination of anti-E-cadherin antibody (13 μg/ml; Abcam, Inc.) and 10 μg/ml Alexa 647-labeled MST-HN or H435A mutants in 1% BSA/PBS at pH 6.5. Bound anti-E-cadherin was detected using Alexa 488-labeled goat anti-rat IgG (Invitrogen/Molecular Probes). Following washes, sections were mounted in Prolong (Invitrogen/Molecular Probes) and imaged using a Zeiss Axiovert 200M epifluorescence microscope with a CCD 12-bit Hamamatsu camera.

Serum levels of human IgG1 (MST-HN or H435A) were analyzed 30 and 90 min following injection of mice using sandwich ELISAs. In brief, 96-well plates were coated with goat anti-human IgG (gamma chain specific; Zymed Laboratories/Invitrogen), blocked with 1% BSA/PBS, and serum samples added at different dilutions. Bound human IgGs were detected using goat anti-human IgG (Fab specific; Sigma) conjugated to HRP.

Data Collection and Analysis for Immunohistochemistry. Sections were sequentially imaged using a Zeiss Axiovert 200M inverted microscope, a Zeiss 63×, 1.4 NA Plan-Apochromat objective, and the following filter sets: exciter HQ470/40×, dichroic Q495LP, emitter HQ525/50 for Alexa Fluor 488; exciter HQ640/20X, dichroic Q660LP, emitter HQ700/75m for Alexa Fluor 647.

Imaging data were processed and displayed using the custom written microscopy image analysis tool (MIATool) software package (www4.utsouthwestern.edu/wardlab/) in MATLAB (Mathworks). The acquired images were embedded in 16-bit gray-scale image formats and overlaid for presentation. The intensities of acquired images were piecewise linearly adjusted. For each organ, the images for Alexa Fluor 647 (MST-HN and H435A mutants) were adjusted using the same parameters. Images were exported into Canvas 10 (ACD Systems of America) for final composition of the figures. No additional intensity adjustments were carried out in Canvas.

Flow Cytometry. Single-cell suspensions were generated from splenocytes and red blood cells lysed as in ref. 4. Cells were incubated in PBS with anti-FcγRIIB/III (2.4G2) or isotype control (rat IgG2b) for 20 min on ice and subsequently in IgG-depleted (5) phenol red-free cDMEM containing 5 μg/ml Alexa 647-labeled MST-HN or H435A mutants for 20 min at 37 °C. Following washes, cells were incubated on ice with the following fluorescently labeled antibodies to identify cell subsets: FITC-labeled anti-CD11b, FITC-labeled anti-CD19, PE-labeled anti-CD11c, PE-or PerCP-labeled anti-B220, PerCP-labeled anti-Gr1, PerCP-labeled anti-CD4 from BD Pharmingen and PE-labeled anti-F4/80 from Invitrogen. Stained cells were analyzed by flow cytometry using a FACSCalibur (BD Biosciences) and FlowJo software (Tree Star, Inc.). Cell populations

were identified as follows: B cells, $B220^+$ or $B220^+CD19^+$; CD4 T cells, $CD4^+$; macrophages, $CD11b^{int}F4/80^+$; monocytes, $CD11b^{hi}Gr\text{-}1^{lo}$, with monocytes identified by analyzing FSC vs. SSC; myeloid DCs (mDCs), $CD11b^+CD11c^+B220^-$.

Pharmacokinetics. Antibodies (IgA, IgG1, H435A, and MST-HN) were radiolabeled with Iodogen as described in ref. 6. Mice were injected with radiolabeled Ig, and remaining radioactivity was analyzed at the indicated times by whole-body counting (7). To determine β-phase half-lives, data were fitted to a decaying biexponential model using custom written software in MATLAB (Mathworks).

Analyses of Serum IgG and Albumin Levels. IgG levels in sera of mice were determined by sandwich ELISA using rabbit anti-mouse IgG (gamma chain specific; Zymed/Invitrogen) and rabbit anti-mouse IgG (heavy and light chain specific; Zymed/Invitrogen) conjugated to HRP and methods previously described by us (8). Serum albumin levels were analyzed using mouse albumin ELISA quantitation kits (Bethyl Laboratories).

1. Foote J, Winter G (1992) Antibody framework residues affecting the conformation of the hypervariable loops. *J Mol Biol* 224:487–499.
2. Chaudhury C, *et al.* (2003) The major histocompatibility complex-related Fc receptor for IgG (FcRn) binds albumin and prolongs its lifespan. *J Exp Med* 197:315–322.
3. Brachtendorf G, *et al.* (2001) Early expression of endomucin on endothelium of the mouse embryo and on putative hematopoietic clusters in the dorsal aorta. *Dev Dyn* 222:410–419.
4. Minguela A, *et al.* (2007) Feedback regulation of murine autoimmunity via dominant anti-inflammatory effects of interferon gamma. *J Immunol* 178:134–144.
5. Ober RJ *et al.* (2004) Visualizing the site and dynamics of IgG salvage by the MHC class I-related receptor, FcRn. *J Immunol* 172:2021–2029.
6. Kim JK, Tsen MF, Ghetie V, Ward ES (1994) Identifying amino acid residues that influence plasma clearance of murine IgG1 fragments by site-directed mutagenesis. *Eur J Immunol* 24:542–548.
7. Vaccaro C, *et al.* (2006) Divergent activities of an engineered antibody in murine and human systems have implications for therapeutic antibodies. *Proc Natl Acad Sci USA* 103:18709–18714.
8. Vaccaro C, Zhou J, Ober RJ, Ward ES (2005) Engineering the Fc region of immunoglobulin G to modulate in vivo antibody levels. *Nat Biotechnol* 23:1283–1288.

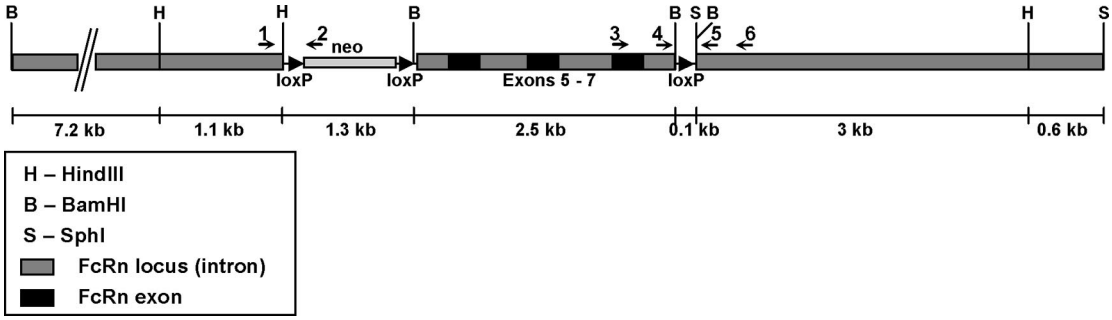

Fig. S1. Strategy for the typing of ES cell recombinants and mice. Schematic representations of FcRn allele (9) following homologous recombination with targeting construct. Neo, neomycin gene. The priming sites of the oligonucleotides used to analyze the presence of different FcRn alleles (wild type; allele with floxed FcRn generated by homologous recombination; and allele with Cre-mediated deletion of exons 5–7 of FcRn) are numbered 1–6.

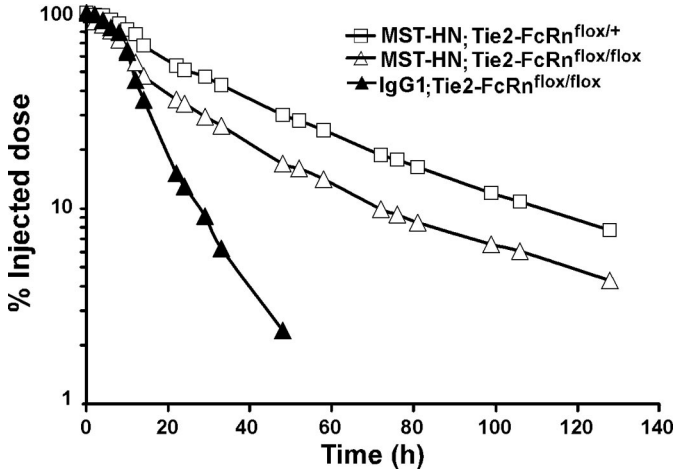

Fig. S2. Clearance of the MST-HN mutant in Tie2-FcRn$^{flox/flox}$ and Tie2-FcRn$^{flox/+}$ mice. Mice were injected with ^{125}I-labeled MST-HN, and radioactivity levels assessed at the indicated times. Data shown represent means of 3 mice (Tie2-FcRn$^{flox/flox}$) or 4 mice (Tie2-FcRn$^{flox/+}$). For comparison, the clearance curve for wild-type IgG1 in Tie2-FcRn$^{flox/flox}$ mice (shown in Fig. 4) is also presented. Data for Tie2-FcRn$^{flox/flox}$ mice are derived from a subset of the total numbers of mice shown in Table 1.